Dynamical bipartite and tripartite entanglement of mechanical oscillators in an optomechanical array

X. Z. Hao,[1] X. Y. Zhang,[1,*] Y. H. Zhou,[2] Wenlin Li,[3] S. C. Hou,[1] and X. X. Yi[4,†]
[1]Department of Physics, Dalian Maritime University, Dalian 116026, China
[2]Quantum Information Research Center, Shangrao Normal University, Shangrao 334000, China
[3]School of Science and Technology, Physics Division, University of Camerino, I-62032 Camerino (MC), Italy
[4]Center for Quantum Sciences and School of Physics, Northeast Normal University, Changchun 130024, China

(Received 6 September 2021; accepted 8 November 2021; published 16 November 2021)

We theoretically propose a method to generate tripartite entanglement of three mechanical oscillators in an optomechanical array. We consider a system comprised of three bichromatically driven optomechanical systems which are coupled to each other via Coulomb interaction of the mechanical oscillators. We show that, for small Coulomb coupling strength, steady tripartite entanglement of the three mechanical oscillators with time periodicity can be generated due to the combined effect of the two-tone drivings and the Coulomb coupling. At large Coulomb coupling strength, the tripartite entanglement exhibits steady entanglement sudden death and revival. The duration of entanglement death during one period can be controlled by the Coulomb coupling strength. The tripartite entanglement is robust against the mechanical thermal noise. Our paper provides us a route for exploring and exploiting controllable and robust multipartite entanglement among macroscopic mechanical oscillators.

DOI: 10.1103/PhysRevA.104.053515

I. INTRODUCTION

Quantum entanglement [1] is one of the most fascinating features of quantum physics and has attracted considerable attention in quantum technologies due to its numerous futuristic potential applications in quantum communication and quantum networks [2–5], quantum metrology [6–9], and fundamental tests of quantum mechanics [10–13]. To date quantum entanglement has been demonstrated in a variety of quantum systems, including superconducting circuits [14–17], atomic ensembles [18,19], and quantum optical setups [20–23]. Cavity optomechanical systems [24], where mechanical modes interact with electromagnetic modes via radiation pressure, could be an alternative platform to realize continuous variable entanglement. Due to the generic radiation-pressure coupling, many proposals have been put forward to generate photon-phonon entanglement [25–29] and photon-photon entanglement [30–32]. The generation of tripartite entanglement has also been investigated in multimode optomechanical systems [33–36] and hybrid optomechanical systems [37,38].

Furthermore, macroscopic mechanical entanglement, which is helpful for clarifying the boundary between the classical world and the quantum world [39] and sensing forces with ultrahigh precision [40], can also be achieved via cavity optomechanical systems. Many different methods have been proposed to entangle two mechanical oscillators, e.g., light-to-matter entanglement transfer [41,42], using time-modulated pump or coupling [43–45], exploiting optical measurement [46–49], and the reservoir engineering based schemes [50–52]. However, these methods mainly focus on bipartite entanglement between two mechanical oscillators; the quantum multipartite entanglement in more complex systems consisting of three or more mechanical oscillators, which has potential applications in multimode quantum information processes [53–58] and investigating quantum many-body phenomena of macroscopic elements [59–63], is barely investigated.

Recently, the authors in Ref. [64] have proposed a method to generate tripartite photonic entanglement by injecting a coupled waveguide array with single-mode squeezed light. Then, one may ask whether this method can be implemented to mechanical oscillators to generate genuine tripartite entanglement of mechanical oscillators. However, injection of a single-mode squeezed state for mechanical oscillators is very difficult. So, we put this question another way, i.e., whether genuine tripartite entanglement of mechanical oscillators can be generated by coupling three independently squeezed mechanical oscillators. The answer is yes. In this paper, we investigate the tripartite entanglement of three mechanical oscillators which are coupled to each other via Coulomb interaction. In order to squeeze each mechanical oscillator independently, we adopt the mechanical squeezing scheme proposed in Ref. [65], i.e., coupling each mechanical oscillator to an optical cavity which is driven bichromatically. We model the dynamics of the system by exploiting the standard Langevin formalism, simulate the linearized dynamics exactly, and investigate the asymptotic dynamics of entanglement for the mechanical modes. In addition to the tripartite entanglement, we also investigate bipartite entanglement be-

*zhangxingyuan1@foxmail.com
†yixx@nenu.edu.cn

 ©2021 American Physical Society

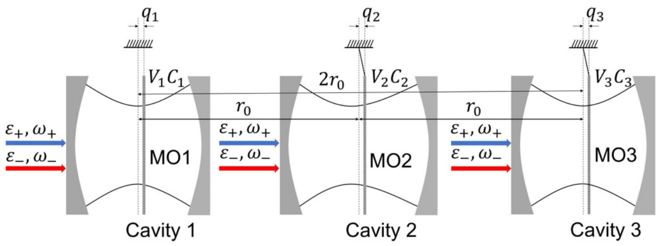

FIG. 1. Schematic diagram of the optomechanical system. It includes three identical optical cavities and three mechanical oscillators. There is no interaction among the cavities. The jth mechanical oscillator (MOj with $j = 1, 2, 3$) couples to the jth cavity by radiation pressure. The jth mechanical oscillator is charged by a bias gate with voltage V_j and capacitance C_j. The three mechanical oscillators couple to each other through Coulomb interaction.

tween any two mechanical oscillators and find that bipartite and tripartite entanglement can occur simultaneously among the three mechanical oscillators. In contrast to the situation of mechanical squeezing where counter-rotating, off-resonant terms associated with the two-tone optical driving fields can be neglected, both the off-resonant terms associated with the bichromatic optical driving and the mechanical Coulomb coupling cannot be ignored in order to achieve large bipartite and tripartite entanglement of the mechanical oscillators. So the mechanical entanglement generated by our method exhibits steady periodic oscillation in the long-time limit. The physical mechanism for the generation of bipartite and tripartite entanglement is that the optical modes can squeeze the phononic supermodes formed by the Coulomb coupling and the squeezed state of the three phononic supermodes is a genuine tripartite entangled state for the three mechanical oscillators. Besides the periodic asymptotic oscillation of mechanical entanglement, when the Coulomb coupling strength crosses a critical value both the bipartite and tripartite entanglement can exhibit stable periodic sudden death and revival, which is of general interest in quantum physics [66,67]. The tripartite entanglement generated in our model can be an order of magnitude larger than that of Ref. [38].

The remainder is organized as follows. In Sec. II, we give the physical model considered in this paper and derive the differential equation satisfied by the covariance matrix of the system. By simulating the differential equation corresponding to the covariance matrix, the asymptotic dynamics of the mechanical entanglement for the three mechanical oscillators is investigated in Sec. III. The dependence of the generated mechanical entanglement on the squeezing parameter and Coulomb coupling strength is also studied in this section. Section V summarizes our results.

II. THEORETICAL MODEL

As depicted in Fig. 1, the system under consideration is comprised of three identical optical cavities, each with one mechanical oscillator. Each optical cavity is driven bichromatically and the mechanical oscillators are coupled through Coulomb interaction. There is no direct interaction among the cavities. The full Hamiltonian of the system is given by

$$\begin{aligned}\hat{H} &= \sum_{j=1}^{3}(\hat{H}_{om,j} + \hat{H}_{dr,j}) + \hat{H}_c,\\ \hat{H}_{om,j} &= \hbar\omega_c\hat{a}_j^\dagger\hat{a}_j + \hbar\omega_m\hat{b}_j^\dagger\hat{b}_j - \hbar g_0\hat{a}_j^\dagger\hat{a}_j(\hat{b}_j^\dagger + \hat{b}_j),\\ \hat{H}_{dr,j} &= \hbar\left(\varepsilon_+e^{-i\omega_+t} + \varepsilon_-e^{-i\omega_-t}\right)\hat{a}_j^\dagger + \text{H.c.},\\ \hat{H}_c &= \hbar(\lambda_{12}\hat{q}_1\hat{q}_2 + \hbar\lambda_{13}\hat{q}_1\hat{q}_3 + \hbar\lambda_{23}\hat{q}_2\hat{q}_3),\end{aligned} \tag{1}$$

where $\hat{a}_j$ and $\hat{b}_j$ are the annihilation operators of the optical mode and mechanical mode in the jth cavity, respectively. ω_c is the optical frequency of the three optical cavities. For simplicity, we have assumed that the three mechanical oscillators are identical so that they have the same effective mass m and the same frequency ω_m. Each mechanical oscillator couples to its own cavity by radiation pressure with the same coupling strength $g_0 = \omega_c/L$. L is the length of the cavities. Every cavity is bichromatically driven by two lasers with frequency $\omega_\pm = \omega_l \pm \omega_m$ and driving amplitude $\varepsilon_\pm$. $\hat{q}_j = (\hat{b}_j + \hat{b}_j^\dagger)/\sqrt{2}$ is the dimensionless position operator of the jth mechanical oscillator. $\hat{H}_c$ represents the Coulomb coupling of the three mechanical oscillators. Under the condition that the distance between the mechanical oscillators is much larger than the displacement of each mechanical oscillator, the Coulomb coupling strengths can be written as [68–70]

$$\frac{\lambda_{12}}{q_{\text{zpf}}^2} = \frac{Q_1Q_2}{2\pi\varepsilon_0r_0^3},\quad \frac{\lambda_{23}}{q_{\text{zpf}}^2} = \frac{Q_2Q_3}{2\pi\varepsilon_0r_0^3},\quad \frac{\lambda_{13}}{q_{\text{zpf}}^2} = \frac{Q_1Q_3}{16\pi\varepsilon_0r_0^3},$$

where r_0 is the equilibrium distance between adjacent mechanical oscillators and $q_{\text{zpf}} = \sqrt{\hbar/2m\omega_m}$ is the zero-point fluctuation of the mechanical oscillators. The charge taken by each mechanical oscillator can be adjusted by an external bias voltage at an electrode on each mechanical oscillator [71]. The charge taken by the jth mechanical oscillator is $Q_j = C_jV_j$, where V_j and C_j are the voltage and the capacitance of the bias gate, respectively. As the charges taken by each mechanical oscillator can be tuned independently, we assume the three Coulomb coupling strengths are the same, i.e., $\lambda_{12} = \lambda_{13} = \lambda_{23} = \lambda$. This can be achieved by setting $Q_1 = Q_3 = 8Q_2$. The Langevin equations of the system in the frame rotating with the frequency ω_l is given by

$$\begin{aligned}\dot{\hat{a}}_j &= -\left\{\frac{\kappa}{2} + i[\Delta_c - g_0(\hat{b}_j^\dagger + \hat{b}_j)]\right\}\hat{a}_j\\ &\quad - i(\varepsilon_{j+}e^{-i\omega_mt} + \varepsilon_{j-}e^{i\omega_mt}) + \sqrt{\kappa}\hat{a}_{j,\text{in}},\\ \dot{\hat{b}}_j &= -\left[\frac{\gamma}{2} + i\omega_m\right]\hat{b}_j + ig_0\hat{a}_j^\dagger\hat{a}_j - i\frac{\lambda}{2}\sum_{k\neq j}(\hat{b}_k^\dagger + \hat{b}_k)\\ &\quad + \sqrt{\gamma}\hat{b}_{j,\text{in}},\end{aligned} \tag{2}$$

where $j = 1, 2, 3$ and $\Delta_c = \omega_c - \omega_l$. The notation $\sum_{k\neq j}$ denotes that k goes from 1 to 3 except the value of j. In addition, κ and γ characterize the decay rates of the optical cavities and the mechanical oscillators, respectively. The zero-mean-value noise operators $\hat{a}_{j,\text{in}}$ and $\hat{b}_{j,\text{in}}$ that describe, respectively, the quantum vacuum noise of the jth cavity and the thermal noise of the jth mechanical oscillator satisfy the commutation relations [72]

$$[\hat{a}_{j,\mathrm{in}}(t), \hat{a}^{\dagger}_{j',\mathrm{in}}(t')] = [\hat{b}_{j,\mathrm{in}}(t), \hat{b}^{\dagger}_{j',\mathrm{in}}(t')] = \delta_{jj'}\delta(t-t')$$

and nonzero correlation functions

$$\begin{aligned}\langle \hat{a}_{j,\mathrm{in}}(t)\hat{a}^{\dagger}_{j',\mathrm{in}}(t')\rangle &= \delta_{jj'}\delta(t-t'),\\ \langle \hat{b}^{\dagger}_{j,\mathrm{in}}(t)\hat{b}_{j',\mathrm{in}}(t')\rangle &= n_{\mathrm{th}}\delta_{jj'}\delta(t-t'),\end{aligned} \tag{3}$$

where $n_{\mathrm{th}} = \{\exp[\hbar\omega_m/(k_B T)] - 1\}^{-1}$ is the mean thermal phonon number of the mechanical oscillators at temperature T with k_B being the Boltzmann constant. This means that all the mechanical oscillators stay at the same environmental temperature. The environmental temperatures of the optical modes are zero. In the limit of large driving fields, the quantum dynamics of the system can be efficiently studied by linearizing the Langevin equations. In this case, the average field amplitudes for both the cavities and the mechanical oscillators are large and the field operators $\hat{a}_j$ and $\hat{b}_j$ can be decomposed as [73–75]

$$\begin{aligned}\hat{a}_j(t) &= \alpha_j(t) + \delta\hat{a}_j,\\ \hat{b}_j(t) &= \beta_j(t) + \delta\hat{b}_j,\end{aligned} \tag{4}$$

where $\alpha_j(t) = \langle \hat{a}_j\rangle$ and $\beta_j(t) = \langle \hat{b}_j\rangle$. $\delta\hat{a}_j$ and $\delta\hat{b}_j$ are the quantum fluctuation operators of the jth optical mode and jth mechanical mode, respectively. We can get the dynamical equations for $\alpha_j(t)$ and $\beta_j(t)$ by taking the average over the quantum Langevin equations (2). Under the mean-field approximation, the classical equations for $\alpha_j(t)$ and $\beta_j(t)$ can be written as

$$\begin{aligned}\dot{\alpha}_j &= -\Big[\frac{\kappa}{2} + i\Delta_{c,j}\Big]\alpha_j - i(\varepsilon_{j+}e^{-i\omega_m t} + \varepsilon_{j-}e^{i\omega_m t}),\\ \dot{\beta}_j &= -\Big[\frac{\gamma}{2} + i\omega_m\Big]\beta_j + ig_0|\alpha_j|^2 - i\frac{\lambda}{2}\sum_{k\neq j}(\beta_k^* + \beta_k),\end{aligned} \tag{5}$$

with $\Delta_{c,j} = \Delta_c - g_0(\beta_j^* + \beta_j)$. By substituting Eq. (4) into the Langevin equations and using Eq. (5), the linearized Langevin equations of the system, in the interaction picture with respect to the Hamiltonian $\hat{H}_0 = \sum_{j=1}^{3}\omega_m\hat{b}_j^{\dagger}\hat{b}_j$, are given by

$$\begin{aligned}\delta\dot{\hat{a}}_j &= -\Big[\frac{\kappa}{2} + i\Delta_{c,j}(t)\Big]\delta\hat{a}_j + \sqrt{\kappa}\hat{a}_{j,\mathrm{in}}\\ &\quad + ig_0\alpha_j(t)(\delta\hat{b}_j^{\dagger}e^{i\omega_m t} + \delta\hat{b}_j e^{-i\omega_m t}),\\ \delta\dot{\hat{b}}_j &= -\frac{\gamma}{2}\delta\hat{b}_j + ig_0[\alpha_j^*(t)\delta\hat{a}_j + \alpha_j(t)\delta\hat{a}_j^{\dagger}]e^{i\omega_m t}\\ &\quad - i\frac{\lambda}{2}\sum_{k\neq j}\big(\delta\hat{b}_k^{\dagger}e^{2i\omega_m t} + \delta\hat{b}_k\big) + \sqrt{\gamma}\hat{b}_{j,\mathrm{in}}.\end{aligned} \tag{6}$$

In order to quantify the entanglement of the mechanical oscillators, we first introduce the standard definition of the optical and mechanical mode quadratures $\hat{x}_j = (\delta\hat{a}_j^{\dagger} + \delta\hat{a}_j)/\sqrt{2}$, $\hat{y}_j = i(\delta\hat{a}_j^{\dagger} - \delta\hat{a}_j)/\sqrt{2}$, $\hat{q}_j = (\delta\hat{b}_j^{\dagger} + \delta\hat{b}_j)/\sqrt{2}$, and $\hat{p}_j = i(\delta\hat{b}_j^{\dagger} - \delta\hat{b}_j)/\sqrt{2}$. The linearized Langevin equations (6) can be expressed in the following compact matrix form:

$$\dot{\mathbf{u}}(t) = \mathbf{M}(t)\mathbf{u}(t) + \mathbf{n}(t), \tag{7}$$

where we have defined the vector of quadrature operators $\mathbf{u} = [\mathbf{v}_1, \mathbf{v}_2, \mathbf{v}_3]^T$ with $\mathbf{v}_j = [\hat{x}_j, \hat{y}_j, \hat{q}_j, \hat{p}_j]$. $\mathbf{n}(t) = [\mathbf{v}_{1,\mathrm{in}}, \mathbf{v}_{2,\mathrm{in}}, \mathbf{v}_{3,\mathrm{in}}]^T$ is the corresponding vector of the noise quadratures with $\mathbf{v}_{j,\mathrm{in}} = [\sqrt{\kappa}\hat{x}_{j,\mathrm{in}}, \sqrt{\kappa}\hat{y}_{j,\mathrm{in}}, \sqrt{\gamma}\hat{q}_{j,\mathrm{in}}, \sqrt{\gamma}\hat{p}_{j,\mathrm{in}}]$. The noise quadratures are $\hat{x}_{j,\mathrm{in}} = (\hat{a}^{\dagger}_{j,\mathrm{in}} + \hat{a}_{j,\mathrm{in}})/\sqrt{2}$, $\hat{y}_{j,\mathrm{in}} = i(\hat{a}^{\dagger}_{j,\mathrm{in}} - \hat{a}_{j,\mathrm{in}})/\sqrt{2}$, $\hat{q}_{j,\mathrm{in}} = (\hat{b}^{\dagger}_{j,\mathrm{in}} + \hat{b}_{j,\mathrm{in}})/\sqrt{2}$, and $\hat{p}_{j,\mathrm{in}} = i(\hat{b}^{\dagger}_{j,\mathrm{in}} - \hat{b}_{j,\mathrm{in}})/\sqrt{2}$. The drift matrix can be written as

$$\mathbf{M}(t) = \begin{pmatrix}\mathbf{B}_1 & \mathbf{C} & \mathbf{C}\\ \mathbf{C} & \mathbf{B}_2 & \mathbf{C}\\ \mathbf{C} & \mathbf{C} & \mathbf{B}_3\end{pmatrix}.$$

The blocks $\mathbf{B}_j$ ($j = 1, 2, 3$) and $\mathbf{C}$ are

$$\mathbf{B}_j = \begin{pmatrix} -\frac{\kappa}{2} & \Delta_{c,j} & -2g_0\mathrm{Im}[\alpha_j]\cos(\omega_m t) & -2g_0\mathrm{Im}[\alpha_j]\sin(\omega_m t)\\ -\Delta_{c,j} & -\frac{\kappa}{2} & 2g_0\mathrm{Re}[\alpha_j]\cos(\omega_m t) & 2g_0\mathrm{Re}[\alpha_j]\sin(\omega_m t)\\ -2g_0\mathrm{Re}[\alpha_j]\sin(\omega_m t) & -2g_0\mathrm{Im}[\alpha_1]\sin(\omega_m t) & -\frac{\gamma}{2} & 0\\ 2g_0\mathrm{Re}[\alpha_j]\cos(\omega_m t) & 2g_0\mathrm{Im}[\alpha_j]\cos(\omega_m t) & 0 & -\frac{\gamma}{2}\end{pmatrix},$$

$$\mathbf{C} = \begin{pmatrix} 0 & 0 & 0 & 0\\ 0 & 0 & 0 & 0\\ 0 & 0 & \frac{\lambda}{2}\sin(2\omega_m t) & \frac{\lambda}{2}[1-\cos(2\omega_m t)]\\ 0 & 0 & -\frac{\lambda}{2}[1+\cos(2\omega_m t)] & -\frac{\lambda}{2}\sin(2\omega_m t)\end{pmatrix}.$$

Re[·] and Im[·] denote the real and imaginary part, respectively. Due to the linearization of the Langevin equations and the Gaussian nature of the quantum noises, the Gaussian nature of the system can be well preserved if the initial state of the system is Gaussian. This means that the quantum dynamics of the system can be completely determined by its 12×12 covariance matrix $\mathbf{V}(t)$, with the matrix elements given by

$$\mathbf{V}_{k,l}(t) = \langle \mathbf{u}_k\mathbf{u}_l + \mathbf{u}_l\mathbf{u}_k\rangle/2. \tag{8}$$

From Eq. (7) and Eq. (8), the linear differential equation satisfied by $\mathbf{V}(t)$ can be written as

$$\dot{\mathbf{V}}(t) = \mathbf{M}(t)\mathbf{V}(t) + \mathbf{V}(t)\mathbf{M}^T(t) + \mathbf{D}, \tag{9}$$

where the diagonal matrix $\mathbf{D}$ is defined as $\mathbf{D}_{k,l}\delta(t-t') = \langle \mathbf{n}_k\mathbf{n}_l + \mathbf{n}_l\mathbf{n}_k\rangle/2$. Using Eq. (3), the matrix $\mathbf{D}$ is $\mathbf{D} = \mathrm{diag}[\mathbf{N}, \mathbf{N}, \mathbf{N}]$ with $\mathbf{N} = [\kappa/2, \kappa/2, \gamma(2n_{\mathrm{th}}+1)/2, \gamma(2n_{\mathrm{th}}+1)/2]$. In the following, we investigate the exact dynamics of the entanglement among the mechanical oscillators by simulating Eq. (9) numerically. The numerical method we use combines two steps: (1) we get the classical dynamics of $\alpha_j(t)$ and $\beta_j(t)$ by simulating Eq. (5) numerically with the initial condition $\alpha_j(0) = \beta_j(0) = 0$ $(j = 1, 2, 3)$ and (2) in determining the dynamics of the covariance matrix, we plug the numerical result of $\alpha_j(t)$ and $\beta_j(t)$ into the drift matrix and simulate Eq. (9). With the exact time evolution of the covariance matrix, we can get the dynamics of the entanglement among the mechanical oscillators. In order to make the following results experimentally achievable, we choose the following set of parameters, which are accessible experimentally, for our numerical simulations [68]: $\omega_c = 2.82 \times 10^5$ GHz, $\omega_m = 2\pi \times 947 \times 10^3$ Hz, $\kappa = 2\pi \times 215 \times 10^3$ Hz, the quality factor $Q = \frac{\omega_m}{\gamma} = 6700$, $m = 145$ ng, and $L = 25$ mm.

III. DYNAMICAL ENTANGLEMENT OF THE MECHANICAL OSCILLATORS

As the driving terms in Eq. (5) are periodic, the asymptotic solutions $\alpha_j(t \to \infty) = \alpha_{j,\mathrm{st}}(t)$ and $\beta_j(t \to \infty) = \beta_{j,\mathrm{st}}(t)$ are periodic. In order to get more insight of the generation of mechanical entanglement, we solve Eq. (5) approximately to get the asymptotic solutions of $\alpha_j(t)$ and $\beta_j(t)$. The asymptotic solutions can be calculated by expanding $\alpha_j(t)$ and $\beta_j(t)$ in powers of g_0. Under the condition that $g_0|\alpha_{j,\mathrm{st}}(t)|$, $g_0|\beta_{j,\mathrm{st}}(t)|$, $\kappa, \lambda \ll \omega_m$, the expansion can be safely kept to the first order in g_0 and the asymptotic solutions $\alpha_{j,\mathrm{st}}(t)$ and $\beta_{j,\mathrm{st}}(t)$ can be approximately written as

$$\begin{aligned} \alpha_{j,\mathrm{st}}(t) &= \alpha_+ e^{-i\omega_m t} + \alpha_- e^{i\omega_m t}, \\ \beta_{j,\mathrm{st}}(t) &= \beta_{\mathrm{dc}} + \beta_+ e^{-2i\omega_m t} + \beta_- e^{2i\omega_m t}, \end{aligned} \tag{10}$$

where the formulas of $\alpha_\pm$, β_{dc}, and $\beta_\pm$ are given in Appendix A 1. As the driving amplitudes of the three cavities are the same, the asymptotic solutions $\alpha_{j,\mathrm{st}}(t)$ and $\beta_{j,\mathrm{st}}(t)$ are independent of j. The details for the derivation of Eq. (10) are left to Appendix A 1. As the phase of $\alpha_\pm$ can be tuned freely through the phase of $\varepsilon_\pm$, we assume that $\alpha_\pm$ are real. The physical mechanism for the generation of the mechanical entanglement can be understood from the linearized Hamiltonian of the system. By using Eq. (10), the linearized Hamiltonian of the system can be written as

$$\begin{aligned} \hat{H}_{\mathrm{lin}} = &\left[\frac{\lambda}{2}\big(\delta\hat{b}_1^\dagger\delta\hat{b}_2 + \delta\hat{b}_1^\dagger\delta\hat{b}_3 + \delta\hat{b}_2^\dagger\delta\hat{b}_3\big) - \sum_{j=1}^{3}\big(G_+\delta\hat{b}_j + G_-\delta\hat{b}_j^\dagger\big)\delta\hat{a}_j + \mathrm{H.c.}\right] \\ &+ \left[\frac{\lambda}{2}\big(\delta\hat{b}_1\delta\hat{b}_2 + \delta\hat{b}_1\delta\hat{b}_3 + \delta\hat{b}_2\delta\hat{b}_3\big)e^{-2i\omega_m t} - \sum_{j=1}^{3}\big(G_+\delta\hat{b}_j^\dagger e^{2i\omega_m t} + G_-\delta\hat{b}_j e^{-2i\omega_m t}\big)\delta\hat{a}_j + \mathrm{H.c.}\right]. \end{aligned} \tag{11}$$

The many-photon optomechanical couplings are $G_\pm = g_0\alpha_\pm$. In Eq. (6), the effective cavity detuning $\Delta_{c,j} = \Delta_c - g_0[\beta_j^*(t) + \beta_j(t)]$ is time periodic in the long-time limit. However, the oscillation amplitude of $\Delta_{c,j}$ is much smaller than ω_m. For the parameters considered in this work, the oscillation amplitude is about $10^{-3}\omega_m$. This means that we can omit the oscillation of $\beta_{j,\mathrm{st}}(t)$. So the effective cavity detuning can be approximated as $\tilde{\Delta}_c = \Delta_c - 2g_0\mathrm{Re}[\beta_{\mathrm{dc}}]$. As Δ_c can be turned freely, we set $\tilde{\Delta}_c = 0$ for all the simulations in this paper for simplification. The terms in the first line represent the resonant term and the terms in the second line describe the off-resonant term. By setting $\lambda = 0$, the above Hamiltonian reduces to the Hamiltonian in Ref. [65], i.e., each cavity squeezes its own mechanical oscillator. In order to see how the entanglement is generated by the resonant term, we define three phononic supermodes and three photonic supermodes, i.e.,

$$\begin{aligned} \hat{d}_1 &= \frac{1}{\sqrt{3}}\big(\delta\hat{b}_1 + \delta\hat{b}_2 + \delta\hat{b}_3\big), \\ \hat{d}_2 &= \frac{1}{\sqrt{2}}\big(\delta\hat{b}_3 - \delta\hat{b}_1\big), \quad \hat{d}_3 = \frac{1}{\sqrt{2}}\big(\delta\hat{b}_2 - \delta\hat{b}_1\big), \end{aligned}$$

$$\begin{aligned} \hat{c}_1 &= \frac{1}{\sqrt{3}}(\delta\hat{a}_1 + \delta\hat{a}_2 + \delta\hat{a}_3), \\ \hat{c}_2 &= \frac{1}{\sqrt{2}}(\delta\hat{a}_3 - \delta\hat{a}_1), \quad \hat{c}_3 = \frac{1}{\sqrt{2}}(\delta\hat{a}_2 - \delta\hat{a}_1). \end{aligned}$$

It should be noted that, although the three cavities do not couple to each other, we can still define three photonic supermodes, following the definition of the phononic supermodes, to diagonalize the resonant term into three uncoupled parts. In terms of $\hat{c}_j$ and $\hat{d}_j$, the resonant term of the linearized Hamiltonian can be written as

$$\hat{H}_R = \sum_{j=1}^{3}\omega_j\hat{d}_j^\dagger\hat{d}_j - \sum_{j=1}^{3}\big[\big(G_+\hat{d}_j + G_-\hat{d}_j^\dagger\big)\hat{c}_j + \mathrm{H.c.}\big], \tag{12}$$

with $\omega_1 = \lambda$ and $\omega_2 = \omega_3 = -\lambda/2$. By setting $G_+ = \mathcal{G}\sinh(r)$ and $G_- = \mathcal{G}\cosh(r)$, the interaction term between the phononic and photonic supermodes becomes $\mathcal{G}\sum_{j=1}^{3}(\hat{\zeta}_j^\dagger\hat{c}_j + \mathrm{H.c.})$ with the Bogoliubov modes $\hat{\zeta}_j = \hat{d}_j\cosh(r) + \hat{d}_j^\dagger\sinh(r)$. This means that $\hat{c}_j$ can cool the Bogoliubov mode $\hat{\zeta}_j$ to vacuum state, which is the squeezed state of $\hat{d}_j$. $\mathcal{G}$ characterizes the cooling rate at which the photonic supermodes cool the Bogoliubov modes and r is the squeezing parameter of the three phononic supermodes. The squeezed state of $\hat{d}_j$ is the entangled state of the three mechanical oscillators. So the physical mechanism of our method is that the Coulomb coupling induces three phononic supermodes for the three mechanical oscillators and the optical cavities squeeze the three phononic supermodes. The combined effect of Coulomb coupling and squeezing leads to the large bipartite and tripartite entanglement of the three mechanical oscillators. Under the condition $G_\pm, \lambda \ll \omega_m$, e.g., $G_\pm, \lambda \sim 10^{-2}\omega_m$, the off-resonant term can be neglected and the system can get a steady-state entanglement of the mechanical oscillators. However, the mechanical entanglement generated in this regime is very small. So we have to increase the values of $G_\pm$ and λ, e.g., $G_\pm, \lambda \sim 0.1\omega_m$, to get large entanglement. In this regime, the approximate solution Eq. (10) is still valid, but the off-resonant term cannot be neglected to get the exact time evolution of the mechanical entanglement. The off-resonant term consists of two parts. The first term in the second line of Eq. (11) comes from the counter-rotating term of the Coulomb coupling. Although this term can generate entanglement of the three mechanical oscillators, the entanglement generated by this term is very small due to $\lambda \ll \omega_m$. The main influence of this term is to make the mechanical entanglement oscillate around the value generated by the resonant term. The other off-resonant term originates from the two-tone optical driving. When $G_\pm \sim 0.1\omega_m$, this term cannot only induce the mechanical entanglement to oscillate, but also weaken the entanglement generated by the resonant term.

By substituting Eq. (10) into the drift matrix $\mathbf{M}(t)$, the drift matrix can be decomposed as $\mathbf{M}(t) = \mathbf{M}_s + \mathbf{M}_o(t)$ with

$$\mathbf{M}_s = \begin{pmatrix} \mathbf{B}_s & \mathbf{C}_s & \mathbf{C}_s \\ \mathbf{C}_s & \mathbf{B}_s & \mathbf{C}_s \\ \mathbf{C}_s & \mathbf{C}_s & \mathbf{B}_s \end{pmatrix}, \quad \mathbf{M}_o(t) = \begin{pmatrix} \mathbf{B}_o & \mathbf{C}_o & \mathbf{C}_o \\ \mathbf{C}_o & \mathbf{B}_o & \mathbf{C}_o \\ \mathbf{C}_o & \mathbf{C}_o & \mathbf{B}_o \end{pmatrix}.$$

The blocks $\mathbf{B}_j$ and $\mathbf{C}_j$ ($j = s, o$) are

$$\mathbf{B}_s = \begin{pmatrix} -\kappa/2 & 0 & 0 & \mathcal{G}_- \\ 0 & -\kappa/2 & \mathcal{G}_+ & 0 \\ 0 & \mathcal{G}_- & -\gamma/2 & 0 \\ \mathcal{G}_+ & 0 & 0 & -\gamma/2 \end{pmatrix},$$

$$\mathbf{B}_o = \begin{pmatrix} \mathbf{0} & \mathbf{B}_{c,o} \\ \mathbf{B}_{m,o} & \mathbf{0} \end{pmatrix},$$

$$\mathbf{C}_s = \begin{pmatrix} \mathbf{0} & \mathbf{0} \\ \mathbf{0} & \mathbf{C}_{\lambda,s} \end{pmatrix}, \quad \mathbf{C}_o = \begin{pmatrix} \mathbf{0} & \mathbf{0} \\ \mathbf{0} & \mathbf{C}_{\lambda,o} \end{pmatrix},$$

with

$$\mathbf{C}_{\lambda,s} = \begin{pmatrix} 0 & \lambda/2 \\ -\lambda/2 & 0 \end{pmatrix},$$

$$\mathbf{B}_{c,o} = \begin{pmatrix} \mathcal{G}_- \sin(2\omega_m t) & -\mathcal{G}_- \cos(2\omega_m t) \\ \mathcal{G}_+ \cos(2\omega_m t) & \mathcal{G}_+ \sin(2\omega_m t) \end{pmatrix},$$

$$\mathbf{B}_{m,o} = \begin{pmatrix} -\mathcal{G}_+ \sin(2\omega_m t) & -\mathcal{G}_- \cos(2\omega_m t) \\ \mathcal{G}_+ \cos(2\omega_m t) & -\mathcal{G}_- \sin(2\omega_m t) \end{pmatrix},$$

$$\mathbf{C}_{\lambda,o} = \frac{\lambda}{2}\begin{pmatrix} \sin(2\omega_m t) & -\cos(2\omega_m t) \\ -\cos(2\omega_m t) & -\sin(2\omega_m t) \end{pmatrix}.$$

The parameters $\mathcal{G}_\pm$ are $\mathcal{G}_\pm = G_+ \pm G_-$ and the effective cavity detuning has been set to zero. $\mathbf{0}$ is 2×2 zero matrix, all the elements of which are zero. The terms $\mathbf{M}_s$ and $\mathbf{M}_o(t)$ result from the resonant part and the off-resonant part of Eq. (11), respectively. From the formula of $\mathbf{M}_o(t)$, we can see that, in the asymptotic regime, the drift matrix oscillates periodically with frequency $2\omega_m$. Hence, in long-time limit, the mechanical entanglement generated by the method also exhibits periodic behavior with period π/ω_m.

To investigate bipartite entanglement of the three mechanical oscillators, we adopt the logarithmic negativity [76–78], which can be readily computed from the reduced covariance matrix of the two mechanical oscillators under consideration. Due to the symmetry of the Hamiltonian Eq. (1), i.e., invariance of the Hamiltonian under any exchange of the subscript j, the bipartite entanglement of any two mechanical oscillators are the same. So we only consider the bipartite entanglement of the first two mechanical oscillators in this work. Consider the following reduced covariance matrix of the two mechanical modes:

$$\mathbf{V}_m = \begin{pmatrix} \mathbf{V}_1 & \mathbf{V}_c \\ \mathbf{V}_c^T & \mathbf{V}_2 \end{pmatrix},$$

where $\mathbf{V}_1$, $\mathbf{V}_2$, and $\mathbf{V}_c$ are 2×2 matrices. $\mathbf{V}_1$ and $\mathbf{V}_2$ represent the local properties of the first and second mechanical oscillator, respectively, while $\mathbf{V}_c$ accounts for the intermode correlations. Then, the logarithmic negativity is given by

$$E_N = \max\{0, -\ln 2\eta\},$$

with

$$\eta = 2^{-1/2}\sqrt{\Sigma(\mathbf{V}_m) - \sqrt{\Sigma(\mathbf{V}_m)^2 - 4\det(\mathbf{V}_m)}},$$
$$\Sigma(\mathbf{V}_m) = \det(\mathbf{V}_1) + \det(\mathbf{V}_2) - 2\det(\mathbf{V}_c).$$

For the study of tripartite entanglement of the mechanical oscillators, we adopt quantitative measures of the residual contangle $\mathcal{R}_\tau$ [79], i.e.,

$$\mathcal{R}_\tau^{b_i|b_jb_k} = C_{b_i|b_jb_k} - C_{b_i|b_j} - C_{b_i|b_k}, \tag{13}$$

with $i, j, k = 1, 2, 3$. $C_{\mu|\nu}$ is the contangle of subsystems μ and ν and is defined as the squared logarithmic negativity. It should be noted that the subsystem ν can contain one or two modes. The contangle $C_{\mu|\nu}$ is the continuous variable analog of the tangle for qubit systems. It has been proved that, for all three-mode Gaussian states, the residual contangle satisfies the monogamy inequality of quantum entanglement [79–81], $\mathcal{R}_\tau^{b_i|b_jb_k} \geqslant 0$, i.e.,

$$C_{b_i|b_jb_k} \geqslant C_{b_i|b_j} + C_{b_i|b_k}, \tag{14}$$

which is analogous to the Coffman-Kundu-Wootters monogamy inequality for systems of three qubits [82]. If all the three residual contangles of a three-mode Gaussian state are nonzero, the Gaussian state is fully inseparable and possesses genuine tripartite entanglement. The monogamy inequality Eq. (14) for continuous variable systems leads naturally to the minimum residual contangle as a *bona fide* quantification of tripartite entanglement [38,80–82], i.e.,

$$\mathcal{R}_\tau^{\min} \equiv \min\left[\mathcal{R}_\tau^{b_1|b_2b_3}, \mathcal{R}_\tau^{b_2|b_1b_3}, \mathcal{R}_\tau^{b_3|b_1b_2}\right], \tag{15}$$

which ensures that $\mathcal{R}_\tau^{\min}$ is monotone under local operations and classical communication. More details of calculating Eq. (15) could be found in Appendix A 2. A nonzero minimum residual contangle indicates the appearance of genuine tripartite entanglement among the three mechanical oscillators. So both the dynamics of the bipartite and tripartite entanglement can be investigated via simulating the dynamics of the covariance matrix of the system.

In Figs. 2(a) and 2(b), we plot the asymptotic dynamics of E_N and $\mathcal{R}_\tau^{\min}$ evaluated with different drift matrix $\mathbf{M}(t)$. From this figure, we can see that the result evaluated with

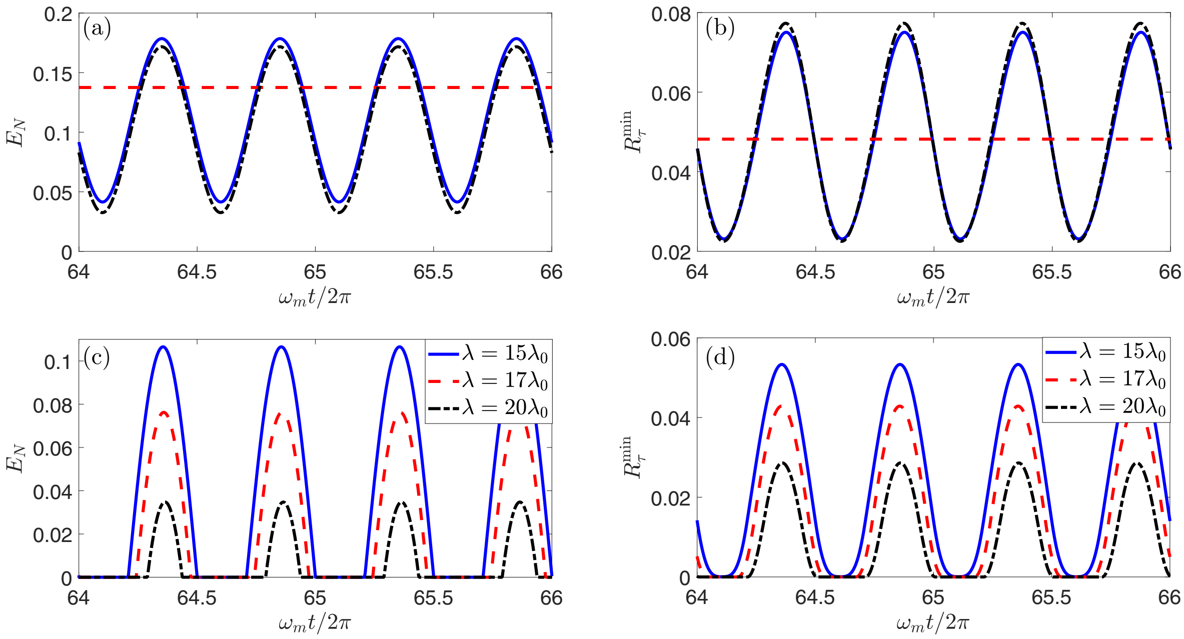

FIG. 2. (a),(b) Comparison of the asymptotic dynamics of E_N and $\mathcal{R}_\tau^{\min}$ evaluated with different drift matrix $\mathbf{M}(t)$. The blue solid lines are evaluated with $\mathbf{M}(t)$ calculated by exactly simulating Eq. (5). The black dash-dotted lines are evaluated with $\mathbf{M}(t) = \mathbf{M}_s + \mathbf{M}_o(t)$. The red dashed lines are evaluated with $\mathbf{M}(t) = \mathbf{M}_s$. (c),(d) Time evolution of E_N and $\mathcal{R}_\tau^{\min}$ in the long-time limit with $\mathbf{M}(t)$ calculated by exactly simulating Eq. (5) for different λ. In (a) and (b), the Coulomb coupling strength is $\lambda = 10\lambda_0$. Other parameters are $\mathcal{G} = 0.1\omega_m$, $r = 0.4$, $n_{\rm th} = 0.5$, and $\lambda_0 = \tilde{\lambda}_0 q_{\rm zpf}^2 = 0.0082\omega_m$ with $\tilde{\lambda}_0 = 8 \times 10^{35}$ Hz/m^2.

exactly simulated $\mathbf{M}(t)$ and the result evaluated with $\mathbf{M}(t) = \mathbf{M}_s + \mathbf{M}_o(t)$ fit well. These two results oscillate around the result obtained with $\mathbf{M} = \mathbf{M}_s$. The oscillation period of E_N and $\mathcal{R}_\tau^{\min}$ is π/ω_m because the oscillation frequency of $\mathbf{M}_o(t)$ is $2\omega_m$. This means that the entanglement is generated mainly by $\mathbf{M}_s$. The term $\mathbf{M}_o(t)$ induces the oscillation of E_N and $\mathcal{R}_\tau^{\min}$ and can impair the entanglement generated by $\mathbf{M}_s$. This confirms the previous discussion. From this figure, we can also see that the bipartite and tripartite entanglement are maximized at the same moments in time. This is in contrast with the monogamy for system of three qubits, the bipartite and tripartite entanglement of which cannot be maximized simultaneously. The reason for this variance is due to the fact that the Hamiltonian Eq. (1) of the system is invariant under any exchange of the subscript j and the reduced state of the three mechanical oscillators is a fully symmetric three-mode Gaussian state which is invariant under the exchange of any two mechanical modes. It has been proved that maximum of the genuine tripartite entanglement and the bipartite entanglement can be achieved simultaneously in fully symmetric three-mode Gaussian states [79]. This phenomenon, which has no counterpart in discrete variable systems, is named as promiscuous sharing of continuous variable entanglement [81]. Figures 2(c) and 2(d) show the exact asymptotic time evolution of E_N and $\mathcal{R}_\tau^{\min}$, respectively, with different λ. From this figure, we can see that, for large λ, both E_N and $\mathcal{R}_\tau^{\min}$ can exhibit periodic vanishing, which is known as entanglement sudden death and revival [66,67,74,83]. The reason for this phenomenon is that, when λ is large, the off-resonant term associated with the Coulomb coupling can induce large oscillation amplitude for E_N and $\mathcal{R}_\tau^{\min}$. When the oscillation amplitude of E_N ($\mathcal{R}_\tau^{\min}$) is equal to the central value of E_N ($\mathcal{R}_\tau^{\min}$), periodic sudden death of bipartite (tripartite) entanglement appears. From these figures, we can also see that the duration of entanglement death in one period increases and the maximum values of the bipartite and tripartite entanglement oscillation decrease as λ increases. When the duration of entanglement death in one period is equal to the oscillation period of the mechanical entanglement, i.e., π/ω_m, the mechanical entanglement of the three mechanical oscillators disappears. This means that the duration of entanglement death can be controlled by the Coulomb coupling strength.

As both the bipartite and tripartite entanglement are periodic in the long-time limit, we identify the degree of the mechanical entanglement with the maximum over one oscillation period, i.e.,

$$E_{N,\max} = \max_{t\in[\mathcal{T},\mathcal{T}+\pi/\omega_m]}\{E_N(t)\},$$

$$\mathcal{R}_{\tau,\max}^{\min} = \max_{t\in[\mathcal{T},\mathcal{T}+\pi/\omega_m]}\{\mathcal{R}_\tau^{\min}(t)\},$$

with $\mathcal{T} \gg 1/\kappa, 1/\gamma$. In Fig. 3(a), we plot $\mathcal{R}_{\tau,\max}^{\min}$ and $E_{N,\max}$ as a function of the squeezing parameter r. From this figure, we can see that $E_{N,\max}$ and $\mathcal{R}_{\tau,\max}^{\min}$ go up first and then go down as r increases. This is because, for small r, the squeezing effect of the cavities on the phononic supermodes, i.e., the resonant terms, is dominant and large bipartite and tripartite entanglement of the mechanical oscillators can be generated. In this regime, the detrimental effect of $\mathbf{M}_o(t)$ is weak and the cavities can squeeze the three phononic supermodes efficiently. For large r, the detrimental effect of $\mathbf{M}_o(t)$ is so strong that it can weaken the squeezing effect of the photonic supermodes. Hence the mechanical entan-

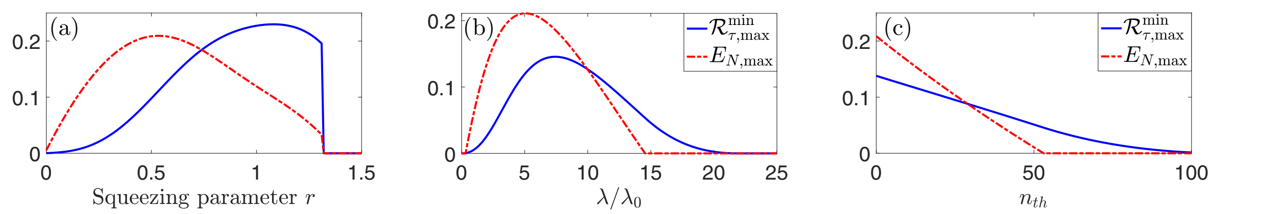

FIG. 3. (a) $\mathcal{R}^{\min}_{\tau,\max}$ (blue solid line) and $E_{N,\max}$ (red dash-dotted line) as a function of the squeezing parameter r with $\lambda = 6\lambda_0$. (b) $\mathcal{R}^{\min}_{\tau,\max}$ and $E_{\tau,\max}$ as a function of the Coulomb coupling strength λ with $r = 0.6$. (c) $\mathcal{R}^{\min}_{\tau,\max}$ and $E_{N,\max}$ as a function of the mechanical mean thermal phonon number $n_{\rm th}$. In (c), the Coulomb coupling strength and the squeezing parameter are $\lambda = 6\lambda_0$ and $r = 0.6$, respectively. Other parameters are the same as Fig. 2.

glement decreases for large r. Figure 3(a) also shows that, when r crosses a critical value, $\mathcal{R}^{\min}_{\tau,\max}$ and $E_{N,\max}$ drop to zero abruptly. This is because, in this regime, the cavities drive the mechanical oscillators into self-sustained oscillation [84] and the asymptotic solution Eq. (10) breaks down. Hence, in this regime, the cavities cannot squeeze the phononic supermodes and both the bipartite and tripartite entanglement of the mechanical oscillators disappear. From this figure, we can also see that, when r is small (large), the bipartite entanglement is larger (smaller) than the tripartite entanglement. Whether the tripartite entanglement is smaller or larger than the bipartite entanglement depends on how the entanglement is distributed among the three mechanical oscillators. From the definition of residual contangle Eq. (13), the residual contangle, e.g., $\mathcal{R}^{b_i|b_j b_k}_{\tau}$, contains two parts. One is $C_{b_i|b_j b_k}$, which represents the entanglement of the $(1+2)$-mode Gaussian state of the (1×2)-mode partition for the state of the three mechanical oscillators. The other one is $C_{b_i|b_j}$ ($C_{b_i|b_k}$), which represents the bipartite entanglement of the reduced two-mode state of the mechanical modes b_i and b_j (b_k). If the entanglement of the system is mainly couplewise entanglement between any pair of modes, $C_{b_i|b_j b_k}$ is not much larger than $C_{b_i|b_j} + C_{b_i|b_k}$. In this situation, the tripartite entanglement is smaller than the bipartite entanglement. However, if the entanglement of the $(1+2)$-mode Gaussian state of the (1×2)-mode partition dominates, $C_{b_j|b_j b_k}$ is much larger than $C_{b_i|b_j} + C_{b_i|b_k}$ and the tripartite entanglement is larger than the bipartite entanglement.

We plot $\mathcal{R}^{\min}_{\tau,\max}$ and $E_{N,\max}$ as a function of λ in Fig. 3(b). From this figure, we can see that both $\mathcal{R}^{\min}_{\tau,\max}$ and $E_{N,\max}$ increase first and then decrease as λ increases. This is because the Coulomb coupling induces a frequency shift for the three phononic supermodes; see Eq. (12). When $\lambda/2 \ll G_\pm$, the interaction term in Eq. (12) can be seen as near resonant and the photonic supermodes can squeeze the phononic supermodes efficiently. When $\lambda \sim G_\pm$, the interaction between the photonic and phononic supermodes in Eq. (12) is largely detuned. In this case, the squeezing effect of the optical modes on the phononic supermodes is weakened and the entanglement of the three mechanical oscillators decreases. As λ increases further, both the bipartite and tripartite entanglement decrease to zero. The dependence of $\mathcal{R}^{\min}_{\tau,\max}$ and $E_{N,\max}$ on the mechanical mean thermal phonon number is exhibited in Fig. 3(c). Although $\mathcal{R}^{\min}_{\tau,\max}$ and $E_{N,\max}$ decrease monotonically with the increase of $n_{\rm th}$, both the bipartite and tripartite entanglement can survive up to large $n_{\rm th}$. The robustness of the bipartite and tripartite entanglement is due to the cooling effect of the optical modes on the Bogoliubov modes formed by the three phononic modes. Even though the temperature of the mechanical oscillators is high, the optical modes can still cool the Bogoliubov modes into a low temperature and squeezing of the three phononic supermodes can be formed. Hence bipartite and tripartite entanglement of the three mechanical oscillators can be generated for large $n_{\rm th}$.

IV. EXPERIMENTAL FEASIBILITY

The key of our protocol is to realize the Coulomb interaction of the mechanical oscillators. Coulomb coupling of mechanical oscillators can be achieved in parallel suspended nanomechanical electrodes [70,71]. The Coulomb coupling strength of the nanomechanical electrodes can be controlled by the bias voltages on the nanomechanical electrodes. In addition, position-position coupling between mechanical oscillators can also be achieved in GaAs-based mechanical oscillators by piezoelectrically induced parametric mode mixing [85]. So, our model can be achieved by putting three nanomechanical electrodes or GaAs-based mechanical oscillators in three optical cavities.

V. CONCLUSION

We have studied the bipartite and tripartite entanglement of three mechanical oscillators in an optomechanical array consisting of three bichromatically driven optomechanical systems. Different sites are coupled through Coulomb coupling between the mechanical oscillators at each site. Due to the combined effect of the two-tone driving fields and the Coulomb coupling, large mechanical bipartite and tripartite entanglement can be generated with experimentally reachable parameters. The asymptotic dynamics of the mechanical entanglement exhibit steady periodic oscillation for small Coulomb coupling strength and show periodic sudden vanishing for large Coulomb coupling strength. The duration of entanglement death during one oscillation period can be controlled by mediating the Coulomb coupling strength. Both the bipartite and tripartite entanglement increase first and then decrease as r increases. The reason is that, for large r, the heating effect of the off-resonant term associated with the bichromatic driving becomes dominant and impairs the entanglement generated by the resonant term. The mechanical entanglement also increases first and then decreases as λ increases. This is because, for large λ, the Coulomb coupling induces a frequency shift for the three phononic supermodes and the resonant term, which is used to squeeze the phononic supermodes, becomes largely detuned. Hence the optical modes cannot squeeze the three phononic supermodes efficiently in the regime of large λ. Both the bipartite and tripartite entanglement generated by our scheme is robust against the mechanical thermal noise. Our scheme provides a tool to explore and exploit robust tripartite entanglement of three mechanical oscillators and can be easily extended to generate multipartite entanglement with more mechanical modes.

ACKNOWLEDGMENTS

This work is supported by the National Natural Science Foundation of China under Grants No. 11775048 and No. 12005032 and the Fundamental Research Funds for the Central Universities under Grant No. 3132021206.

APPENDIX

1. Approximate solutions of $\alpha_j(t)$ and $\beta_j(t)$

In order to get the approximate solutions of Eq. (5), we expand $\alpha_j(t)$ and $\beta_j(t)$ in powers of the small parameter g_0, i.e.,

$$\alpha_j(t)=\sum_{n=0}^{\infty}g_0^n\alpha_j^{(n)}(t),\quad \beta_j(t)=\sum_{n=0}^{\infty}g_0^n\beta_j^{(n)}(t). \quad \text{(A1)}$$

By plugging the equations into Eq. (5), we can get the equations for $\alpha_j^{(n)}(t)$ and $\beta_j^{(n)}(t)$. As the asymptotic solutions are independent of the initial conditions, so we assume initial condition $\alpha_j(0)=\beta_j(0)=0$ $(j=1,2,3)$. The equations for each component of the expansions can be written as

$$\begin{aligned}\dot{\alpha}_j^{(n)}&=-\Big[\frac{\kappa}{2}+i\Delta_c\Big]\alpha_j^{(n)}+i\sum_{l=0}^{n-1}\big(\beta_j^{(l)*}+\beta_j^{(l)}\big)\alpha_j^{(n-l-1)}\\&\quad+\varepsilon^{(n)},\\ \dot{\beta}_j^{(n)}&=-\Big[\frac{\gamma}{2}+i\omega_m\Big]\beta_j^{(n)}+i\sum_{l=0}^{n-1}\alpha_j^{(l)*}\alpha_j^{(n-l-1)}\\&\quad-i\frac{\lambda}{2}\sum_{k\neq j}\beta_k^{(n)},\end{aligned}$$

where $\varepsilon^{(0)}=-i(\varepsilon_+e^{-i\omega_m t}+\varepsilon_-e^{i\omega_m t})$ and $\varepsilon^{(n)}$ with $n\neq 0$ is zero. In the above equations, we have done rotating-wave approximation to the Coulomb interaction as $\lambda\ll\omega_m$. The solutions of the above equations can be computed iteratively. After tedious and straightforward calculations, the expressions for the zero-order and first-order coefficients, in the long-time limit, are given by

$$\begin{aligned}\alpha_{j,\mathrm{st}}^{(0)}(t)&=\alpha_+e^{-i\omega_m t}+\alpha_-e^{i\omega_m t},\\ \beta_{j,\mathrm{st}}^{(0)}(t)&=\alpha_{j,\mathrm{st}}^{(1)}(t)=0,\end{aligned}$$

$$\begin{aligned}\beta_{j,\mathrm{st}}^{(1)}(t)=&\frac{i(|\alpha_+|^2+|\alpha_-|^2)}{\frac{\gamma}{2}+i(\omega_m+\lambda)}+\frac{i\alpha_-^*\alpha_+}{\frac{\gamma}{2}-i(\omega_m-\lambda)}e^{-2i\omega_m t}\\&+\frac{i\alpha_+^*\alpha_-}{\frac{\gamma}{2}+i(3\omega_m+\lambda)}e^{2i\omega_m t},\end{aligned}$$

where

$$\begin{aligned}\alpha_+&=\frac{-i\varepsilon_+}{\frac{\kappa}{2}+i(\Delta_c-\omega_m)},\\ \alpha_-&=\frac{-i\varepsilon_-}{\frac{\kappa}{2}+i(\Delta_c+\omega_m)}.\end{aligned}\quad \text{(A2)}$$

Under the condition $g_0|\alpha_\pm|,\kappa,\lambda\ll\omega_m$, the asymptotic solutions of $\alpha_j(t)$ and $\beta_j(t)$ can be safely expanded at the lowest order in g_0. So the asymptotic solutions of $\alpha_j(t)$ and $\beta_j(t)$ can be approximated as

$$\begin{aligned}\alpha_{j,\mathrm{st}}(t)&=\alpha_+e^{-i\omega_m t}+\alpha_-e^{i\omega_m t},\\ \beta_{j,\mathrm{st}}(t)&=\beta_{dc}+\beta_+e^{-2i\omega_m t}+\beta_-e^{2i\omega_m t},\end{aligned}$$

where

$$\begin{aligned}\beta_{\mathrm{dc}}&=\frac{ig_0(|\alpha_+|^2+|\alpha_-|^2)}{\frac{\gamma}{2}+i(\omega_m+\lambda)},\\ \beta_+&=\frac{ig_0\alpha_-^*\alpha_+}{\frac{\gamma}{2}-i(\omega_m-\lambda)},\\ \beta_-&=\frac{ig_0\alpha_+^*\alpha_-}{\frac{\gamma}{2}+i(3\omega_m+\lambda)}.\end{aligned}$$

2. Calculation of $\mathcal{R}_\tau^{\min}$

The value of $\mathcal{R}_\tau^{b_i|b_jb_k}$ can be calculated as follows. The formula of $\mathcal{R}_\tau^{b_i|b_jb_k}$ is

$$\mathcal{R}_\tau^{b_i|b_jb_k}\equiv C_{b_i|b_jb_k}-C_{b_i|b_j}-C_{b_i|b_k},$$

where $C_{\mu|\nu}=E_{\mu|\nu}^2$ (ν contains one or two modes). $E_{\mu|\nu}$ is the logarithmic negativity between subsystems μ and ν. The *one-mode-vs-one-mode* logarithmic negativity $E_{b_i|b_j}$ is defined as

$$E_{b_i|b_j}\equiv\max[0,-\ln(2\tilde{\nu}_-)],$$

where $\tilde{\nu}_-=\min[\mathrm{eig}(|i\Omega_2\tilde{\mathbf{V}}_m^{(ij)}|)]$ is the minimum symplectic eigenvalue of the covariance matrix $\tilde{\mathbf{V}}_m^{(ij)}=\mathcal{P}_{i|j}\mathbf{V}_m^{(ij)}\mathcal{P}_{i|j}$ with the symplectic matrix $\Omega_2=\oplus_{j=1}^2 i\sigma_y$ (σ_y is the y-Pauli matrix). $\mathbf{V}_m^{(ij)}$ is the reduced covariance matrix of the ith and jth mechanical oscillators and can be obtained by removing in $\mathbf{V}_m$ (the reduced covariance matrix of the three mechanical oscillators) the rows and columns of the uninteresting mode. The matrix $\mathcal{P}_{i|j}$, that realizes partial transposition at the level of the covariance matrix [86], is $\mathcal{P}_{i|j}=\mathrm{diag}(1,-1,1,1)$ for $i<j$ and $\mathcal{P}_{i|j}=\mathrm{diag}(1,1,1,-1)$ for $i>j$. The calculation of the *one-mode-vs-two-modes* logarithmic negativity $E_{b_i|b_jb_k}$ is the same as the calculation of $E_{b_i|b_j}$. To calculate $E_{b_i|b_jb_k}$, one only needs to replace $\Omega_2=\oplus_{j=1}^2 i\sigma_y$ with $\Omega_3=\oplus_{j=1}^3 i\sigma_y$ and $\tilde{\mathbf{V}}_m^{(ij)}=\mathcal{P}_{i|j}\mathbf{V}_m^{(ij)}\mathcal{P}_{i|j}$ with $\tilde{\mathbf{V}}_m=\mathcal{P}_{i|jk}\mathbf{V}_m\mathcal{P}_{i|jk}$, where the partial transposition matrices are $\mathcal{P}_{1|23}=\mathrm{diag}(1,-1,1,1,1,1)$, $\mathcal{P}_{2|13}=\mathrm{diag}(1,1,1,-1,1,1)$, and $\mathcal{P}_{3|12}=\mathrm{diag}(1,1,1,1,1,-1)$.

[1] R. Horodecki, P. Horodecki, M. Horodecki, and K. Horodecki, Rev. Mod. Phys. **81**, 865 (2009).

[2] S. L. Braunstein and P. van Loock, Rev. Mod. Phys. **77**, 513 (2005).

[3] A. Xuereb, C. Genes, and A. Dantan, Phys. Rev. Lett. **109**, 223601 (2012).

[4] R. Rabl, S. J. Kolkowitz, F. H. L. Koppens, J. G. E. Harris, P. Zoller, and M. D. Lukin, Nat. Phys. **6**, 602 (2010).

[5] H. J. Kimble, Nature (London) **453**, 1023 (2008).

[6] D. J. Wineland, J. J. Bollinger, W. M. Itano, F. L. Moore, and D. J. Heinzen, Phys. Rev. A **46**, R6797(R) (1992).

[7] S. F. Huelga, C. Macchiavello, T. Pellizzari, A. K. Ekert, M. B. Plenio, and J. I. Cirac, Phys. Rev. Lett. **79**, 3865 (1997).

[8] V. Giovannetti, S. Lloyd, and L. Maccone, Nat. Photon. **5**, 222 (2011).

[9] C. Chen, L. Jin, and R. B. Liu, New J. Phys. **21**, 083002 (2019).

[10] W. H. Zurek, Rev. Mod. Phys. **75**, 715 (2003).

[11] A. Bassi, K. Lochan, S. Satin, T. P. Singh, and H. Ulbricht, Rev. Mod. Phys. **85**, 471 (2013).

[12] J. Zhang, T. C. Zhang, and J. Li, Phys. Rev. A **95**, 012141 (2017).

[13] B. Julsgaard, A. Kozhekin, and E. S. Polzik, Nature (London) **413**, 400 (2001).

[14] M. Neeley *et al.*, Nature (London) **467**, 570 (2010).

[15] L. DiCarlo, M. Reed, L. Sun, B. L. Johnson, J. M. Chow, J. M. Gambetta, L. Frunzio, S. M. Girvin, M. H. Devoret, and R. J. Schoelkopf, Nature (London) **467**, 574 (2010).

[16] E. Flurin, N. Roch, F. Mallet, M. H. Devoret, and B. Huard, Phys. Rev. Lett. **109**, 183901 (2012).

[17] J. Q. You and F. Nori, Nature (London) **474**, 589 (2011).

[18] J. M. Raimond, M. Brune, and S. Haroche, Rev. Mod. Phys. **73**, 565 (2001).

[19] Y. Guo, X. B. Luo, S. Ma, and C. C. Shu, Phys. Rev. A **100**, 023409 (2019).

[20] T. Aoki, N. Takei, H. Yonezawa, K. Wakui, T. Hiraoka, A. Furusawa, and P. van Loock, Phys. Rev. Lett. **91**, 080404 (2003).

[21] J. W. Pan, Z. B. Chen, C. Y. Lu, H. Weinfurter, A. Zeilinger, and M. Żukowski, Rev. Mod. Phys. **84**, 777 (2012).

[22] S. Armstrong, M. Wang, R. Y. Teh, Q. H. Gong, Q. Y. He, J. Janousek, H. A. Bachor, M. D. Reid, and P. K. Lam, Nat. Phys. **11**, 167 (2015).

[23] L. K. Shalm, D. R. Hamel, Z. Yan, C. Simon, K. J. Resch, and T. Jennewein, Nat. Phys. **9**, 19 (2013).

[24] M. Aspelmeyer, T. J. Kippenberg, and F. Marquardt, Rev. Mod. Phys. **86**, 1391 (2014).

[25] D. Vitali, S. Gigan, A. Ferreira, H. R. Böhm, P. Tombesi, A. Guerreiro, V. Vedral. A. Zeilinger, and M. Aspelmeyer, Phys. Rev. Lett. **98**, 030405 (2007).

[26] C. Genes, A. Mari, P. Tombesi, and D. Vitali, Phys. Rev. A **78**, 032316 (2008).

[27] M. Paternostro, D. Vitali, S. Gigan, M. S. Kim, C. Brukner, J. Eisert, and M. Aspelmeyer, Phys. Rev. Lett. **99**, 250401 (2007).

[28] S. G. Hofer, W. Wieczorek, M. Aspelmeyer, and K. Hammerer, Phys. Rev. A **84**, 052327 (2011).

[29] R. X. Chen, L. T. Shen, and S. B. Zheng, Phys. Rev. A **91**, 022326 (2015).

[30] S. Barzanjeh, D. Vitali, P. Tombesi, and G. J. Milburn, Phys. Rev. A **84**, 042342 (2011).

[31] L. Tian, Phys. Rev. Lett. **110**, 233602 (2013).

[32] Y. D. Wang and A. A. Clerk, Phys. Rev. Lett. **110**, 253601 (2013).

[33] A. Xuereb, M. Barbieri, and M. Paternostro, Phys. Rev. A **86**, 013809 (2012).

[34] X. H. Yang, Y. Ling, X. P. Shao, and M. Xiao, Phys. Rev. A **95**, 052303 (2017).

[35] Y. D. Wang, S. Chesi, and A. A. Clerk, Phys. Rev. A **91**, 013807 (2015).

[36] C. Jiang, S. Tserkis, K. Collins, S. Onoe, Y. Li, and L. Tian, Phys. Rev. A **101**, 042320 (2020).

[37] Y. Xiang, F. X. Sun, M. Wang, Q. H. Gong, and Q. Y. He, Opt. Express **23**, 30104 (2015).

[38] J. Li, S. Y. Zhu, and G. S. Agarwal, Phys. Rev. Lett. **121**, 203601 (2018).

[39] K. Modi, A. Brodutch, H. Cable, T. Paterek, and V. Vedral, Rev. Mod. Phys. **84**, 1655 (2012).

[40] S. Mancini and P. Tombesi, Europhys. Lett. **61**, 8 (2003).

[41] S. Mancini, V. Giovannetti, D. Vitali, and P. Tombesi, Phys. Rev. Lett. **88**, 120401 (2002).

[42] J. Zhang, K. C. Peng, and S. L. Braunstein, Phys. Rev. A **68**, 013808 (2003).

[43] R. X. Chen, L. T. Shen, Z. B. Yang, H. Z. Wu, and S. B. Zheng, Phys. Rev. A **89**, 023843 (2014).

[44] M. Abdi and M. J. Hartmann, New J. Phys. **17**, 013056 (2015).

[45] M. Wang, X. Y. Lü, Y. D. Wang, J. Q. You, and Y. Wu, Phys. Rev. A **94**, 053807 (2016).

[46] S. Pirandola, D. Vitali, P. Tombesi, and S. Lloyd, Phys. Rev. Lett. **97**, 150403 (2006).

[47] K. Børkje, A. Nunnenkamp, and S. M. Girvin, Phys. Rev. Lett. **107**, 123601 (2011).

[48] M. Abdi, S. Pirandola, P. Tombesi, and D. Vitali, Phys. Rev. Lett. **109**, 143601 (2012).

[49] M. J. Woolley and A. A. Clerk, Phys. Rev. A **87**, 063846 (2013).

[50] C. J. Yang, J. H. An, W. L. Yang, and Y. Li, Phys. Rev. A **92**, 062311 (2015).

[51] M. J. Woolley and A. A. Clerk, Phys. Rev. A **89**, 063805 (2014).

[52] M. Asjad, S. Zippilli, and D. Vitali, Phys. Rev. A **93**, 062307 (2016).

[53] M. Roukes, Phys. World **14**, 25 (2001).

[54] K. Stannigel, P. Rabl, A. S. Sørensen, P. Zoller, and M. D. Lukin, Phys. Rev. Lett. **105**, 220501 (2010).

[55] G. Heinrich, M. Ludwig, J. Qian, B. Kubala, and F. Marquardt, Phys. Rev. Lett. **107**, 043603 (2011).

[56] M. Lassen, V. Delaubert, J. Janousek, K. Wagner, H. A. Bachor, P. K. Lam, N. Treps, P. Buchhave, C. Fabre, and C. C. Harb, Phys. Rev. Lett. **98**, 083602 (2007).

[57] F. Massel, T. T. Heikkilä, J. M. Pirkkalainen, S. U. Cho, H. Saloniemi, P. J. Hakonen, and M. A. Sillanpää, Nature (London) **480**, 351 (2011).

[58] X. W. Xu, Y. J. Zhao, and Y. X. Liu, Phys. Rev. A **88**, 022325 (2013).

[59] H. Seok, L. F. Buchmann, S. Singh, and P. Meystre, Phys. Rev. A **86**, 063829 (2012).

[60] M. Ludwig and F. Marquardt, Phys. Rev. Lett. **111**, 073603 (2013).

[61] M. Ludwig, K. Hammerer, and F. Marquardt, Phys. Rev. A **82**, 012333 (2010).

[62] A. Xuereb, C. Genes, and A. Dantan, Phys. Rev. A **88**, 053803 (2013).

[63] A. Tomadin, S. Diehl, M. D. Lukin, P. Rabl, and P. Zoller, Phys. Rev. A **86**, 033821 (2012).
[64] S. Rojas-Rojas, E. Barriga, C. Muñoz, P. Solano, and C. Hermann-Avigliano, Phys. Rev. A **100**, 023841 (2019).
[65] A. Kronwald, F. Marquardt, and A. A. Clerk, Phys. Rev. A **88**, 063833 (2013).
[66] T. Yu and J. H. Eberly, Phys. Rev. Lett. **93**, 140404 (2004).
[67] T. Yu and J. H. Eberly, Science **323**, 598 (2009).
[68] P. C. Ma, J. Q. Zhang, Y. Xiao, M. Feng, and Z. M. Zhang, Phys. Rev. A **90**, 043825 (2014).
[69] X. Y. Zhang, Y. H. Zhou, Y. Q. Guo, and X. X. Yi, Phys. Rev. A **98**, 033832 (2018).
[70] L. Tian and P. Zoller, Phys. Rev. Lett. **93**, 266403 (2004).
[71] W. K. Hensinger, D. W. Utami, H. S. Goan, K. Schwab, C. Monroe, and G. J. Milburn, Phys. Rev. A **72**, 041405(R) (2005).
[72] F. Bemani, R. Roknizadeh, A. Motazedifard, M. H. Naderi, and D. Vitali, Phys. Rev. A **99**, 063814 (2019).
[73] A. Mari and J. Eisert, Phys. Rev. Lett. **103**, 213603 (2009).
[74] C. S. Hu, Z. Q. Liu, Y. Liu, L. T. Shen, H. Z. Wu, and S. B. Zheng, Phys. Rev. A **101**, 033810 (2020).
[75] J. Li, I. M. Haghighi, N. Malossi, S. Zippilli, and D. Vitali, New J. Phys. **17**, 103037 (2015).
[76] G. Vidal and R. F. Werner, Phys. Rev. A **65**, 032314 (2002).
[77] G. Adesso, A. Serafini, and F. Illuminati, Phys. Rev. A **70**, 022318 (2004).
[78] M. B. Plenio, Phys. Rev. Lett. **95**, 090503 (2005).
[79] G. Adesso, A. Serafini, and F. Illuminati, Phys. Rev. A **73**, 032345 (2006).
[80] G. Adesso and F. Illuminati, J. Phys. A **40**, 7821 (2007).
[81] G. Adesso and F. Illuminati, New J. Phys. **8**, 15 (2006).
[82] V. Coffman, J. Kundu, and W. K. Wootters, Phys. Rev. A **61**, 052306 (2000).
[83] C. Joshi, J. Larson, M. Jonson, E. Andersson, and P. Öhberg, Phys. Rev. A **85**, 033805 (2012).
[84] F. Marquardt, J. G. E. Harris, and S. M. Girvin, Phys. Rev. Lett. **96**, 103901 (2006).
[85] H. Okamoto, A. Gourgout, C. Y. Chang, K. Onomitsu, I. Mahboob, E. Y. Chang, and H. Yamaguchi, Nat. Phys. **9**, 480 (2013).
[86] R. Simon, Phys. Rev. Lett. **84**, 2726 (2000).